ChemPhotoChem

Research Article
doi.org/10.1002/cptc.202300107

Chemistry Europe
European Chemical Societies Publishing

www.chemphotochem.org

Electron-Deficient Phenanthrenequinone Derivative for Photoactivated Hydrogen Atom Transfer Mediated Oxidation of Secondary Alcohols

Juulia Talvitie,[a] Iida Alanko,[a] Anna Lenarda,[a] Nikita Durandin,[b] Nikolai Tkachenko,[b] Martin Nieger,[a] and Juho Helaja*[a]

In 2000, Fukuzumi and co-workers reported a seminal study on the photochemical oxidation of benzylic alcohols with visible-light-excited 9,10-phenanthrenequinone (PQ) under argon atmosphere (*J. Am. Chem. Soc.* **2000**, *122*, 8435). We optimized the reaction conditions they reported and were able to oxidize 1-(4-methoxyphenyl)ethanol quantitatively to 4'-methoxyacetophenone in only 15 min with 10 mol% PQ as a photocatalyst under oxygen. However, we observed a significant decrease in the oxidation rate with more electron-deficient benzylic alcohols as starting materials. To improve the photooxidation performance, we designed a high-yielding synthetic route for a novel, more electron-deficient PQ derivative, 3,6-bis(trifluoromethyl)-9,10-phenanthrenequinone (PQ-CF_3). Its efficiency as a photocatalyst in the fast oxidation of secondary alcohols was demonstrated not only with several electronically diverse benzylic alcohols but also with aliphatic substrates. The comprehensive mechanistic studies based on Hammett plot construction, kinetic isotope experiments, and DFT computations suggest that the mechanistic pathway of the alcohol oxidation is dependent on the electronic properties of both the catalyst and the substrate. As the key mechanistic discovery, we showed that the newly developed PQ-CF_3 operates as a highly efficient hydrogen atom transfer (HAT) catalyst.

Introduction

Along with the rise of photoredox catalytic methods during recent years, various oxidative organic transformations employing visible light and atmospheric oxygen have emerged.[1] In these procedures, organophotocatalysts have provided a useful tool for the oxidative activation of organic substrates either via single-electron transfer (SET) or hydrogen atom transfer (HAT). The organocatalyst is subsequently regenerated from its reduced form by triplet oxygen reduction to superoxide. Notably, this process cannot be broadly employed with many common metal-based photocatalysts, as their excited states tend to be quenched by $^3O_2$.[2] Even though organocatalysts normally display lower turnover numbers than metal catalysts, those are well compensated from the affordability and sustainability point of view.[3,4] Moreover, one of the most interesting features of organocatalysts for a photoredox catalysis chemist is their synthetic moldability.[5] As a representative example, Nicewicz's and Sparr's teams have shown that the photophysical and catalytic properties of Fukuzumi-type acridinium salts can be notably adjusted via synthetic tailoring.[6–8] Similarly, the catalytic performance of naphthochromenones[9] and cyanoarenes[10] has been improved by rational design of their structural features.[11]

Among organophotocatalysts, carbonyl compounds form a distinct family for their capability to operate in both SET and HAT processes.[12] Within this group, aromatic dicarbonyl compounds i.e. quinones stand out for their capability to undergo two-electron and two-proton reduction to hydroquinones.[13] Especially excited state anthraquinones have been extensively studied and utilized as oxidative photocatalysts,[14] but over the last few years, 9,10-phenanthrenequinone (PQ) has caught increasing attention. Most of the PQ-catalyzed reactions reported to this date proceed via SET pathway,[15–20] and so far, only a few HAT mediated processes have been developed. A fairly common HAT pathway accessed by visible-light-excited PQ (PQ*) proceeds via the formation of an acyl radical from an aldehyde substrate.[21–23] However, PQ has also been reported to be capable of generating neutral radicals from simple alkanes.[24]

Even though there is a lot of structural variation in photocatalytic anthraquinones,[14] to the best of our knowledge, the photooxidative properties of PQ have not been previously tailored with synthetic modification. Moreover, there is a lack of knowledge on the influence of such structural changes on the mechanistic behavior of PQ. As both ground state and excited state reduction potentials of quinones are known to increase when the electron density on the quinone ring decreases,[25] our

[a] J. Talvitie, I. Alanko, Dr. A. Lenarda, Dr. M. Nieger, Dr. J. Helaja
Department of Chemistry
University of Helsinki
A.I. Virtasen aukio 1, 00014 Helsinki, Finland
E-mail: juho.helaja@helsinki.fi

[b] Dr. N. Durandin, Prof. Dr. N. Tkachenko
Faculty of Engineering and Natural Sciences
Tampere University
33101 Tampere, Finland

Supporting information for this article is available on the WWW under https://doi.org/10.1002/cptc.202300107

goal was to functionalize PQ with electron-withdrawing substituents to improve its oxidative performance. The flat aromatic structure of PQ makes it rather poorly soluble in most organic solvents, and hence, we chose CF_3 moieties for their ability to improve the solubility. Additionally, CF_3 groups are typically unreactive while at the same time being strongly electron-withdrawing.

We selected alcohol oxidation as a simple yet fundamental organic transformation to demonstrate the oxidation ability of our newly developed photocatalyst. In recent years, several completely metal-free photocatalytic methods have emerged to effectively oxidize benzylic alcohols but usually, aliphatic substrates require long reaction times or deliver only moderate yields.[26–32] Most importantly, alcohol oxidation is known to allow mechanistic variability as both SET and HAT mediated methods have been reported.[26–29] Hence, it is possible for PQ to induce the two consecutive dehydrogenations of the alcohol substrate either via SET followed by proton transfer (PT) or via HAT (Scheme 1).

Herein, we report the synthesis and photocatalytic properties of the previously unpublished 3,6-bis(trifluoromethyl)-9,10-phenanthrenequinone (PQ-CF_3) and demonstrate its superior efficacy as a catalytic photooxidant in the oxidation of secondary alcohols in comparison with commercial PQ. Comprehensive experimental and computational mechanistic investigations revealed that PQ catalyzes fast single-electron oxidation with electron-rich benzylic alcohols, while PQ-CF_3 operates as an efficient, HAT-selective photooxidant for all substrates regardless of their electronic properties.

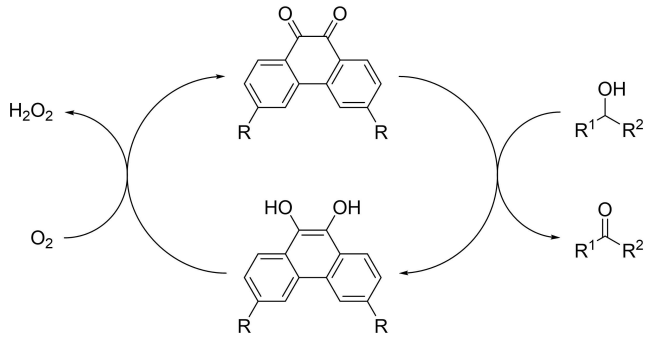

Scheme 1. The oxidation of an alcohol substrate catalyzed by PQ derivative with oxygen as the terminal oxidant.

Results and Discussion

One of the most common synthetic strategies to construct PQ derivatives is the cyclization of a pre-functionalized substrate. Trosien and Waldvogel used $MoCl_5/TiCl_4$ to cyclize benzil derivatives to PQs with excellent yields, but their method was limited to electron-rich substrates.[33] Gradl and co-workers introduced a double Friedel-Crafts to 3,3'-disubstituted biphenyl, receiving a mixture of both 3,6- and 1,6-disubstituted PQ.[34] More recently, Ishikawa and co-workers utilized Suzuki-coupling and subsequent intramolecular N-heterocyclic carbene (NHC) catalyzed benzoin condensation in the synthesis of the PQ derivative picene-13,14-dione.[35] We chose their method to synthesize PQ-CF_3 and received dicarbaldehyde **3** in 70% yield from the homocoupling of 2 equivalents of 2-bromo-4-(trifluoromethyl)benzaldehyde **1**. However, the reaction rapidly produced the dehalogenated 4-(trifluoromethyl)benzaldehyde as a side product. An improved yield of 92% was achieved by preparing the borylated intermediate **2** in a separate step[36] and subsequently coupling it with **1** (Scheme 2). Notably, we were able to lower the Pd catalyst loading in the borylation step from the reported 10 mol% to only 1 mol%, and no purification of **2** was needed prior to the Suzuki-coupling.

Next, we cyclized the obtained dicarbaldehyde **3** to PQ-CF_3 by intramolecular benzoin condensation and subsequent aerobic oxidation. Our attempt to adapt Ishikawa's conditions with 3-ethyl-5-(2-hydroxyethyl)-4-methylthiazolium bromide as the NHC pre-catalyst and DBU as a base[35] resulted in a complex mixture of PQ-CF_3 with several side products. However, Suresh and co-workers used similar conditions in the synthesis of dibenzo[b,f]oxepine-10,11-diones, and their comprehensive pre-catalyst optimization revealed that 1,3-bis(2,4,6-trimethylphenyl)imidazolium chloride (IMesHCl) performed nearly as well as their optimal thiazolium salt.[37] When we carried out the benzoin condensation with 10 mol% IMesHCl and DBU as the base in anhydrous THF, we achieved a clean and complete conversion of **3** to hydroquinone PQH_2-CF_3 already in 30 min.

PQ hydroquinones oxidize normally spontaneously to quinones under aerobic conditions, and hence, a separate oxidation step is not needed.[38,39] However, CF_3 moieties turned out to stabilize the hydroquinone enough for it to survive several weeks in a dilute solution under air. When we attempted to oxidize PQH_2-CF_3 with aerobic oxygen in a concentrated MeCN solution, we obtained a significant amount of 5,5'-bis(trifluoromethyl)-2,2'-dibenzoic acid as a side product. PQ is known to undergo oxidative degradation to dibenzoic acid in the presence of a strong base[40] or an excess of H_2O_2 in

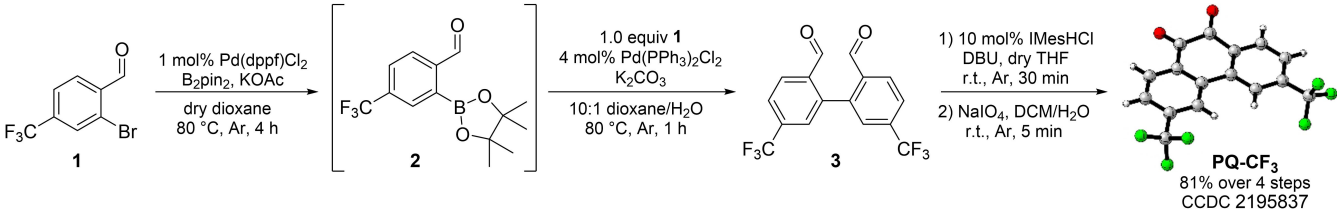

Scheme 2. The developed synthesis of PQ-CF_3.

either acidic or basic conditions.[41] As aerobic oxidation of the hydroquinone produces equimolar amount of H_2O_2,[20] we believe that PQ-CF_3 is prone to oxidative degradation even when a trace amount of H_2O_2 is present in a concentrated solution. When PQH_2-CF_3 was oxidized with $NaIO_4$ under argon,[42] the reaction yielded quickly and selectively PQ-CF_3, resulting in the final yield of 81% over four steps (Scheme 2).

To evaluate the oxidative ability of the newly developed compound, we investigated the photophysical properties of both PQ and PQ-CF_3. Furthermore, we included the 3,6-dimethoxysubstituted derivative PQ-OMe in the comparison to increase variety in the electronic nature of the quinones (Table 1). The ground state reduction potentials E^0_{red} of all three quinones were measured using cyclic voltammetry. The triplet excited state energies of PQ and PQ-CF_3 (ΔE_{0-0}) were determined from the maxima of the phosphorescence spectra (λ_{0-0}), and excited state reduction potentials (E^0_{red}*) were calculated as the sum of the ground state potential and the triplet excited state energy. For PQ-OMe, the literature value of λ_{0-0} was used.[43] Our experimental results were in agreement with the previously reported photophysical properties of PQ.[43,45] Analogously to benzoquinone derivatives,[25] both the ground and excited state reduction potentials increased when more electron-withdrawing substituents were introduced to the phenanthrene backbone.

As PQ's capability to oxidize benzylic alcohols has been already reported,[45] we started optimizing the reaction conditions for the oxidation of 1-(4-methoxyphenyl)ethanol **4a** with PQ as the photocatalyst (Table 2). The initial conditions were adapted from Fukuzumi and co-workers.[45] Toluene proved to be the best solvent (Table 2, entries 7–9), but we chose MeCN for further tests to see if the reaction rate could be improved by addition of water. Interestingly, we observed that the oxidation proceeded drastically faster in MeCN/H_2O. We hypothesize that this is associated with the enhanced PQ regeneration rate in aqueous environment as our experimental observations suggested (SI, Table S1).

Table 1. Experimentally determined photophysical properties of PQ and its derivatives.

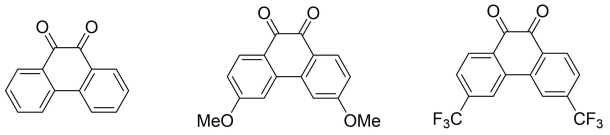

PQ | PQ-OMe | PQ-CF_3

	PQ	PQ-OMe	PQ-CF_3
excitation λ_{max} (nm)	410	343	395
λ_{0-0} (nm)[a]	572	560[43]	582
ΔE_{0-0} (eV)	2.17	2.21	2.13
E^0_{red} vs. SCE (V)[b]	−0.66	−0.81	−0.40
E^0_{red}* vs. SCE (V)	1.51	1.40	1.73
excited state lifetime τ (ms)[a]	6.0	6.5[43]	6.0

[a] Measured in MeCN/CCl_4 at 100 K (SI, Figures S8–S9). [b] Determined by cyclic voltammetry in MeCN vs. Fc/Fc^+ and converted to SCE[44] (SI).

Table 2. Effect of the variation of reaction parameters[a].

4a → 5a

entry	deviation to standard conditions	time (min)	yield[b] (%)
1	none	15	>99 (92)[c]
2	1 mmol **4a** [0.1 M]	120	88[c]
3	no light	60	0
4	no photocatalyst	60	0
5	Ar atmosphere	15	8
6	air atmosphere	15	52
7	acetone as solvent	60	35
8	toluene as solvent	60	60
9	MeCN as solvent	60	26
10	MeCN/H_2O (5:1) as solvent	15	38
11	MeCN/H_2O (9:1) as solvent	15	76
12	5 mol% PQ	15	97
13	5 mol% PQ	30	>99
14	5 mol% Acr^+-Mes ClO_4^-	15	12
15	5 mol% Eosin Y	15	0
16	5 mol% anthraquinone	15	1
17	**4c** instead of **4a**	30	15
18	10 mol% PQ-CF_3 in MeCN/H_2O (7:1)[d]	30	28
19	10 mol% PQ-CF_3 in MeCN/H_2O (5:1)[d]	30	94
20	10 mol% PQ-CF_3 in MeCN/H_2O (4:1)[d]	30	89

[a] The reactions were performed in 0.20 mmol scale. Full reaction optimization in SI, Tables S1–S6. [b] NMR yield, 1,3,5-trimethoxybenzene as an internal standard. [c] Isolated yield after SiO_2 chromatography. [d] 1-Phenylethanol **4c** was used as the starting material.

We noticed that older batches of PQ resulted in lower yields of 4'-methoxyacetophenone **5a**, significantly affecting the reproducibility of the benzylic oxidation. In the recent literature, the source of PQ has been reported to have an effect on its reactivity.[46] Initially, we reasoned that this could be caused by the varying purity level, but both recrystallization and sublimation of commercial PQ only decreased its activity. Therefore, we propose that due to its planar structure, as its degree of crystallinity increases, PQ tends to form aggregates exhibiting a lower catalytic efficacy. Indeed, sonication of the PQ stock solution prior to the reaction enhanced the rate of the alcohol oxidation, restoring the original values and allowing us to obtain reproducible results.

When the MeCN/H_2O ratio was optimized to 7:1 and a sonicated stock solution of PQ was used, a quantitative NMR yield of **5a** was obtained already in 15 min with 10 mol% PQ under oxygen atmosphere. Increasing the scale of the reaction to 1 mmol led to an isolated yield of 88% in 2 h. The catalyst loading could be decreased to 5 mol% to get **5a** quantitatively in 30 min. Control experiments proved that both light and photocatalyst are essential for the reaction to proceed, as well as oxygen atmosphere to efficiently regenerate PQ (Table 2,

entries 3–6). All the other tested organophotocatalysts performed poorly in the oxidation of **4a** (Table 2, entries 14–16). However, 1-phenylethanol **4c** gave only 15% of acetophenone **5c** in the optimized conditions with PQ after 30 min irradiation. Changing the catalyst to the newly developed PQ-CF_3 doubled the yield to 28%. By adjusting the MeCN/H_2O ratio to 5:1 (Table 2, entries 18–20), we achieved **5c** in a 94% yield with 10 mol% of PQ-CF_3 in 30 min. A quantitative yield of **5c** was achieved when the reaction time was prolonged to 1 h.

With the optimized reaction conditions in hand, we started to study the scope of the oxidation of secondary alcohols with PQ-CF_3 as the photocatalyst. Most 4- and 3-substituted benzylic alcohols (**4c**, **4e**, **4h**, **4k**–**l**) as well as other acyclic benzylic alcohols (**4r**, **4t**, **4w**–**y**) gave quantitative yields of the corresponding ketones in 1–4 h (Scheme 3). We performed the oxidation of **4e** also in 1 mmol scale to test the scalability of the reaction with PQ-CF_3 and obtained an isolated yield of 95% after 3 h irradiation.

With the 4-methyl substituted alcohol **4b**, PQ-CF_3 caused partial oxidation of the methyl group, and better selectivity was achieved with PQ. The substrates **4d** and **4f** with acidic moieties seemed to cause oxidative degradation of PQ-CF_3 over prolonged irradiation. Surprisingly, the yield of 3'-methoxyacetophenone **5i** was only 43% even after 18 h irradiation, and the reaction was even slower with PQ. Computational investigations revealed that even though the oxidation potential of **4i** is close to that of **4a**, its radical cation form has practically no LUMO population on the benzylic carbon (SI, Figure S15), which would explain the sluggish reactivity in the SET pathway. 2-Substituted benzylic alcohols **4m**–**p** required longer reaction times and afforded varying yields (31–91%). The yield decreased upon the increasing size of the substituent, suggesting that this behavior was caused by steric hindrance. With cyclic benzylic alcohols **4q** and **4s**, the rigidity of the substrate could be responsible for the lower yields (79% in 18 h and 49% in 4 h, respectively).

To our delight, our system was capable of oxidizing aliphatic secondary alcohols remarkably fast. Cyclohexanone **5aa** was obtained in 80% yield and 2-pentanone **5ac** quantitatively already in 3 h. Aliphatic alcohols **4u** and **4ab** with a bulky substituent on the chain resulted in good yields of ketones **5u** and **5ab** (68% in 8 h and 76% in 4 h, respectively), but surprisingly, cyclohexenone **5z** was produced only in 10% yield in 18 h. In a similar trend to acyclic and cyclic benzylic alcohols, the yield of 2-indanone **5v** was only 6% after 4 h irradiation.

In our attempt to oxidize primary alcohols, we failed to stop the oxidation at the aldehyde stage but received a mixture of aldehyde, carboxylic acid, and peroxy acid instead. We reason that this occurred due to PQ's ability to generate acyl radicals from benzaldehydes,[21,22] which reacted further with oxygen in our conditions leading to the formation of acidic side products. Besides, Zhang's team has recently reported a catalyst-free cross-coupling taking place between PQ-semiquinone and an acyl radical,[47] which would irreversibly deactivate our catalyst.

To gain insight on the mechanistic behavior of PQ and PQ-CF_3, we first performed kinetic measurements with substrate **4c** (Figure 1A). As expected, PQ-CF_3 performed notably faster giving quantitative yield of **5c** in 1 h, whereas PQ produced only 27% yield in the same irradiation period. The role of oxygen as a terminal oxidant was confirmed by the detection of H_2O_2 with UV-Vis spectroscopy (SI). Despite the formation of H_2O_2 in the reaction, oxidative degradation of PQ-CF_3 occurred only when acidic moieties were present on the substrates, or the reaction time was prolonged over 18 h. Next, we carried out the oxidation of substrates **4a** and **4e** in the standard reaction conditions with TEMPO as a radical scavenger (Figure 1B). PQ and PQ-CF_3 were used as catalysts, respectively. A significant decrease in the isolated yields of **5a** and **5e** was obtained, thus confirming the radical nature of the reaction. Furthermore, the oxidation of a radical clock substrate 1-(4-cyclopropylphenyl)ethanol **4ad** produced only 18% of ketone **5ad** during 2 h irradiation even though only 18% of unreacted **4ad** was left in the reaction mixture (Figure 1B). A complex mixture of unidentified side products also formed in the reaction, suggesting that cyclopropyl ring opening occurred during the oxidation.

We carried out Hammett correlation measurements with 4-substituted benzylic alcohols **4a**–**c** and **4e**–**h** by determining

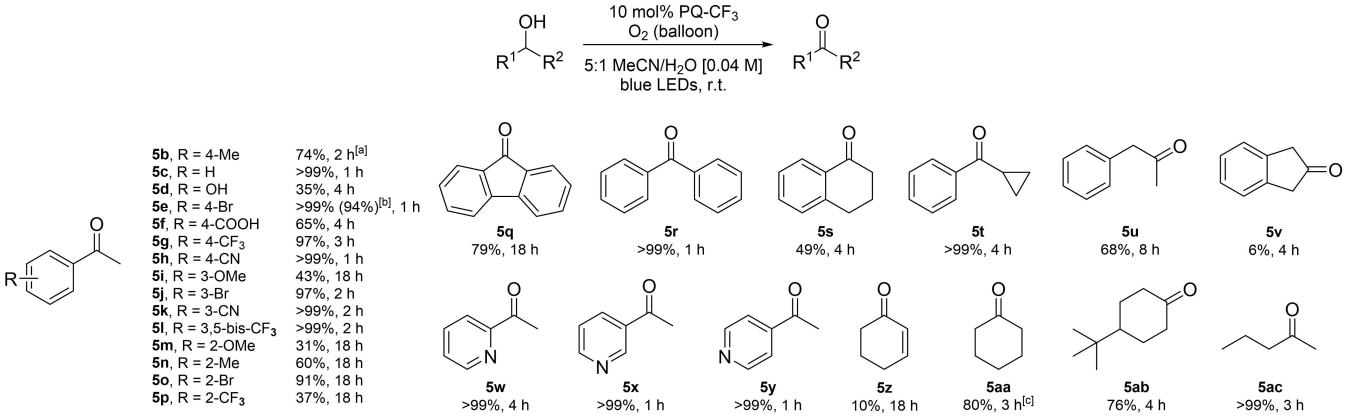

Scheme 3. The scope of the alcohol oxidation. The reactions were performed in 0.20 mmol scale. NMR yields were measured with 1,3,5-trimethoxybenzene as an internal standard. [a] With 10 mol% PQ in 7:1 MeCN/H_2O. [b] Isolated yield after SiO_2 chromatography. [c] The reaction was performed in 0.10 mmol scale in 5:1 CD_3CN/H_2O.

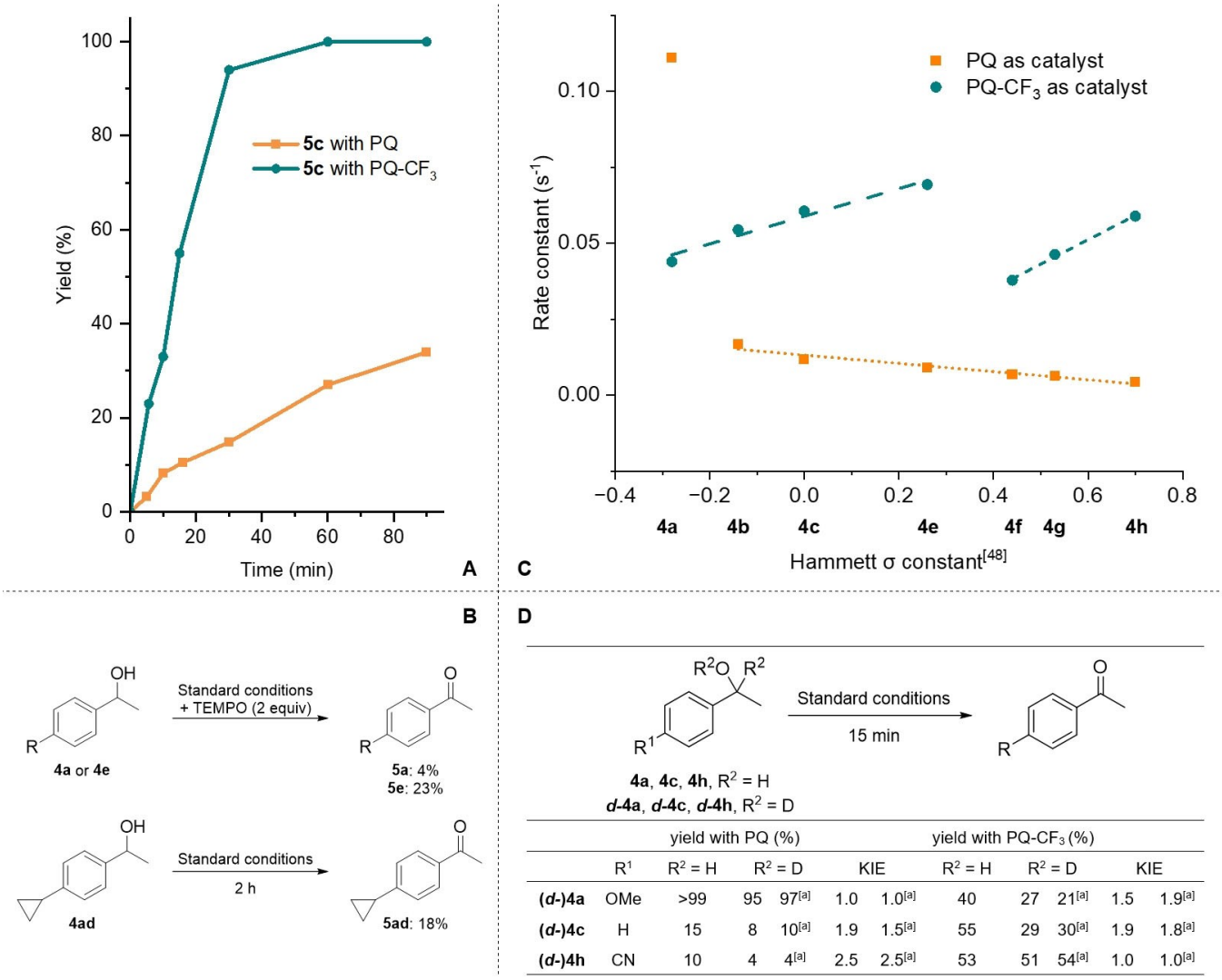

	yield with PQ (%)					yield with PQ-CF_3 (%)				
	R^1	R^2 = H	R^2 = D		KIE	R^2 = H	R^2 = D		KIE	
(*d*-)**4a**	OMe	>99	95	97[a]	1.0	1.0[a]	40	27	21[a]	1.5	1.9[a]
(*d*-)**4c**	H	15	8	10[a]	1.9	1.5[a]	55	29	30[a]	1.9	1.8[a]
(*d*-)**4h**	CN	10	4	4[a]	2.5	2.5[a]	53	51	54[a]	1.0	1.0[a]

Figure 1. Mechanistic investigations. Reactions with PQ were performed in 7:1 MeCN/H_2O and those with PQ-CF_3 in 5:1 MeCN/H_2O. 1,3,5-Trimethoxybenzene was used as an internal standard for the NMR yields. A) Kinetic monitoring of the conversion of **4c** to **5c** with PQ or PQ-CF_3 as a photocatalyst in the standard reaction conditions. A separate reaction was carried out for each time point. B) Experiments with the radical scavenger TEMPO (isolated yields after SiO_2 chromatography) and the radical clock substrate 1-(4-cyclopropylphenyl)ethanol **4ad**. PQ was used with **4a** and PQ-CF_3 with **4e** and **4ad**. C) Observed Hammett correlation with substrates **4a**–**c** and **4e**–**h** using PQ or PQ-CF_3 as a photocatalyst in the standard reaction conditions. Reaction time 15 min. D) The kinetic deuterium isotope effects. The reaction time was 30 min with PQ and 15 min with PQ-CF_3. With 4-MeO-substituted alcohols **4a** and *d*-**4a**, the reaction time was always 15 min. KIE was calculated as k_H/k_D at the fixed time point. [a] D_2O was used instead of H_2O.

the rate constants from the NMR yields measured after 15 min irradiation (Figure 1C). Phenolic substrate **4d** was discarded from the plot as PQ could not oxidize it to **5d**. To get further understanding on the reaction mechanism, we carried out the oxidation of deuterium-labelled alcohols *d*-**4a**, *d*-**4c**, and *d*-**4h** in MeCN/H_2O and MeCN/D_2O (Figure 1D). Furthermore, we performed quantum chemical calculations at DFT level to estimate the oxidation potentials (E^0_{ox}) and bond dissociation enthalpies (BDEs) of alcohols and possible intermediates in the mechanistic pathway to interpret the experimental results (Table 3).

The obtained Hammett correlations were mostly linear, with PQ showing a negative and PQ-CF_3 a positive trend, but additionally, both catalysts showed a point of discontinuity in their respective plots. PQ provided a quantitative conversion of 4-methoxy-substituted **4a** remarkably fast, whereas the other substrates were converted much more slowly, with the reaction rate decreasing as the substrate got more electron-deficient ($\varrho = -0.014$). Fukuzumi's team has previously proposed a SET pathway for the oxidation of **4a** with PQ,[45] and our experimental evidence supports their observations (Scheme 4). The excited state reduction potential of PQ (Table 1) is identical to the oxidation potential of **4a** (Table 3), which makes PQ a strong enough single-electron oxidant for **4a**. However, the oxidation potentials of alcohols **4b**–**c** and **4e**–**h** are much higher, suggesting that PQ is likely to induce their first dehydrogenation via HAT instead of SET.

The benzylic alcohol radical cations **II** forming on the SET pathway (Scheme 4) are known to be strong acids whereas PQ radical anions are strong bases, causing the PT from **II** to occur

Table 3. Computed BDEs and oxidation potentials of 1-(4-R-phenyl)ethanols **4a–c** and **4e–h** and their radical intermediates ordered against Hammett σ_p-values.

	σ_p	BDE[a] kcal/mol	BDE[a] kcal/mol	E^0_{ox} [b] I→II V vs. SCE	E^0_{ox} [b] III→IV V vs. SCE	
4a	−0.28	83.2	30.6	1.51	−0.44	−0.65[c]
4b	−0.11	82.5	32.1	1.92	−0.27	−0.49[c]
4c	0.00	82.3	32.8	2.27	−0.15	−0.40[c]
4e	0.26	82.1	33.3	2.10	−0.07	−0.33[c]
4f	0.44	80.0	36.2	2.46	0.18	−0.07[c]
4g	0.53	81.2	34.9	2.55	0.15	−0.11[c]
4h	0.70	80.1	36.3	2.53	0.24	−0.01[c]

[a] Computed with M06-2X/def2-tzvp in gas phase. [b] Computed with B3LYP/6-31 + (d,p) with CPCM (MeCN). [c] Computed for H-bonded H_2O complex.

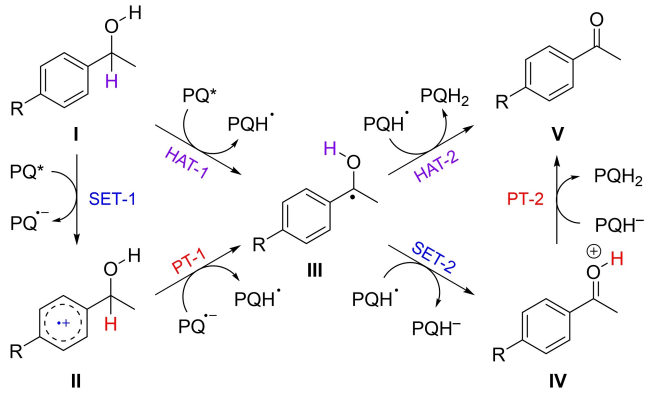

Scheme 4. Possible mechanistic pathways of benzylic alcohol oxidation with visible-light-excited PQ.

fast.[45] Hence, H/D is not involved in the rate-determining step (RDS) on the SET pathway, and the absence of the kinetic isotope effect (KIE) with alcohol ***d*-4a** confirms the proposed mechanism (Figure 1D). Substrates ***d*-4c** and ***d*-4h** on the other hand exhibit significant KIEs, indicating the cleavage of H/D to be a part of the RDS. However, the negative trend in the Hammett plot correlates better with the BDEs of the second HAT rather than the first (Table 3), although the observed KIEs show that changing H_2O to D_2O does not have a notable effect on the reaction rate (Figure 1D). We propose that even though both dehydrogenations occur via HAT (Scheme 4), the latter is the RDS while the first one is a preequilibrium step.[49] This scenario is supported by the increasing O–H BDEs of the neutral radical intermediates **III** upon decreasing electron density (Table 3).

The Hammett plot with PQ-CF_3 displays completely opposite behavior to PQ. Substrates **4a–c** and **4e** have a linear positive correlation ($\varrho = 0.045$) after which there is a point of discontinuity and a parallel upward line ($\varrho = 0.080$) for substrates **4f–h** (Figure 1C). In this case, the oxidation potentials of the alcohols do not provide explanation for the different behavior of PQ and PQ-CF_3, as the excited state reduction potentials of both catalysts are only high enough to exceed the oxidation potential of substrate **4a**. Besides, the oxidation of electron-rich **4a** proceeds notably faster with PQ despite PQ-CF_3 is a stronger photooxidant. This phenomenon could be associated with a change of mechanism from SET to HAT in the first dehydrogenation step (Scheme 4). The positive Hammett correlation is consistent with the decreasing BDEs of the benzylic C–Hs (Table 3), suggesting that the first dehydrogenation would also be the RDS for the more electron-rich substrates with PQ-CF_3. This reasoning is further supported by the observed high KIEs with deuterated substrates ***d*-4a** and ***d*-4c** (Figure 1D). However, the second dehydrogenation may proceed either via HAT or SET, as the alcohol radical intermediates have both weak BDEs and low oxidation potentials (Table 3).

The point of discontinuity in the Hammett plot with PQ-CF_3 indicates a mechanistic change for alcohols **4f–h**. Their oxidation potentials are significantly higher compared to the other substrates, whereas the BDEs of their benzylic C–Hs are even lower (Table 3), making the first dehydrogenation still very likely to occur via HAT instead of SET. However, the observed KIE of 1.0 with 4-CN-substituted ***d*-4h** (Figure 1D) suggests that cleavage of H/D no longer occurs in the RDS. Analogously to the more electron-deficient substrates with PQ, we propose that the RDS with **4f–h** is the second dehydrogenation step which in this case occurs via SET according to the KIE experiments. To get further evidence for our theory, we computed the reduction potential of the semiquinone HPQ-$CF_3^{\bullet}$ (Scheme 5) and found out that it is actually lower than the oxidation potentials of the neutral alcohol radicals **III** formed from substrates **4f–h** (Table 3). However, the formation of H-

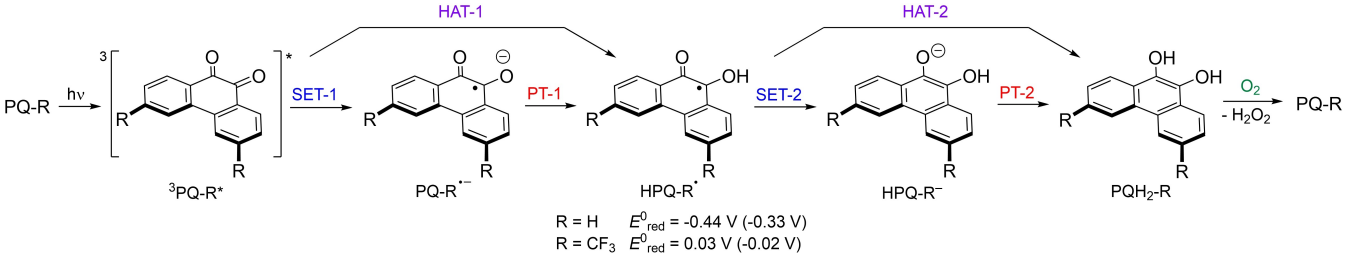

Scheme 5. Detailed redox transformations of PQ derivative during one catalytic cycle. Reduction potentials were computed with B3LYP/6-31 + (d,p) with CPCM (MeCN) vs. SCE. Values in parentheses are computed for the H_2O complex.

bonded H_2O complexes of the radicals **III** turned out to decrease their oxidation potentials below the reduction potential of the semiquinone. Additionally, the computations of alcohol radicals with acetone as a H-bond acceptor revealed that the H-bonding ability of the benzylic radical **III** is stronger the more electron-deficient it is (SI, Table S8), rationalizing the positive Hammett correlation and indicating that the second, rate-determining dehydrogenation operates via proton-coupled electron transfer (PCET) mechanism.[50]

Based on both experimental and computational studies, we propose that the mechanistic pathway of the alcohol oxidation, as well as the RDS, depends on the redox properties of both the substrate and the catalyst of choice (Table 4). According to our findings, PQ-CF_3 appears to be a highly efficient HAT catalyst, whereas PQ displays faster reactivity on the SET pathway. The difference in their catalytic behavior was visualized by computing spin densities and lowest unoccupied molecular orbitals (LUMOs) for the triplet excited states of both catalysts as well as their H_2O complexes (SI, Figures S16–S17). The results indicate that the spin density is delocalized throughout the ring system of PQ*, and this effect is notably reinforced with H_2O. Instead, water has little to no effect on PQ-CF_3* where the spin density is more localized on the carbonyls, explaining PQ-CF_3's higher affinity for H-atoms than for electrons.

Conclusions

In summary, we have developed an efficient synthetic route for a new organophotocatalyst, PQ-CF_3, and studied its photophysical properties in comparison with the previously reported compounds PQ and PQ-OMe. The photocatalytic efficacy of PQ-CF_3 was demonstrated in the oxidation of 29 benzylic and aliphatic alcohols under mild, metal-free conditions in oxygen atmosphere. The mechanistic investigations revealed a switch in the oxidation mechanism from SET to HAT between PQ and PQ-CF_3, which brings PQ-CF_3 forward as an interesting alternative for the current photocatalytic systems traditionally requiring the use of an additional HAT catalyst or mediator.

Experimental Section

General Information. All commercial chemicals were used as received. 9,10-Phenanthrenequinone (98.0%) and $Pd(dppf)Cl_2$ (98.0%) were purchased from Fluorochem. $Pd(PPh_3)_2Cl_2$ (Pd 14.0%min) was purchased from Alfa Aesar. IMesHCl was synthesized according to a known literature procedure.[51] Anhydrous dioxane was dried over 4 Å molecular sieves prior to use. Anhydrous THF was taken from The Vacuum Atmospheres Solvent purification system and used immediately. Glassware was stored in ambient conditions before use unless otherwise specified. The stock solutions of PQ and PQ-CF_3 were sonicated with a Branson 1800 Ultrasonic Cleaner. NMR spectra were recorded at 25 °C on Bruker Avance Neo 400 MHz or 500 MHz spectrometers. [D6]Acetone and TMS-containing $CDCl_3$ were used as deuterated solvents with solvent signals (2.05, 29.84 and 0.00 (from TMS), 77.16 ppm, respectively) as references for chemical shifts. In ^{19}F NMR measurements, $CFCl_3$ (0.00 ppm) was used as a reference. NMR yields were calculated with 1,3,5-trimethoxybenzene as an internal standard. UV-Vis spectra were measured with a Varian Cary 50 UV-Visible spectrophotometer using standard 10 mm glass cuvettes. Thin-layer chromatography (TLC) was conducted using silica gel GF254 with fluorescence indicator (254 nm). Chromatographic separations were performed with VWR silica gel (230–300 mesh). The high-resolution mass spectra (HRMS) were obtained on a Jeol MStation JMS-700 (EI) instrument with a quadrupole mass analyzer. The photoreaction set up is shown in Figure S1 (SI). The light source was 3×3W ProLight Opto royal blue (450–460 nm) LEDs which were positioned on the bottom of the reaction vial at a 4 mm distance. The UV-Vis emission spectrum of the LEDs is shown in Figure S2 (SI). No filters were used. The measured light power of 3 LEDs was 1.03 W. The reaction stand was a custom-made aluminum block with build-in water cooling.

Table 4. The dependence of the proposed RDS on the redox potentials of the substrate and the photocatalyst.

E^0_{ox} of **I**	RDS	E^0_{ox} of **III**	RDS
$\leq E^0_{red}$* of PQ	SET-1	$\leq E^0_{red}$ of HPQ-$CF_3^{\bullet}$	HAT-1
$> E^0_{red}$* of PQ	HAT-2	$> E^0_{red}$ of HPQ-$CF_3^{\bullet}$	SET-2 (PCET)

*Synthesis of 5,5'-Bis(trifluoromethyl)-[1,1'-biphenyl]-2,2'-dicarbaldehyde (**3**).* The two-step synthesis was performed using modified literature procedures.[35,36] An oven-dried two-neck flask was charged with B_2pin_2 (2.53 g, 9.96 mmol, 1.5 equiv), $Pd(dppf)Cl_2$ (49 mg, 0.066 mmol, 1 mol%), and KOAc (1.63 g, 16.6 mmol, 2.5 equiv), and the flask was evacuated and backfilled with argon (three cycles). Anhydrous dioxane (27 mL) and 2-bromo-4-(trifluoromethyl)benzaldehyde **1** (1.0 mL, 6.64 mmol, 1.0 equiv) were added to the flask. The mixture was bubbled with argon for 30 min and stirred at 80 °C in an oil-bath for 4 h, until the reaction was complete according to ^1H NMR. The reaction mixture was cooled down, filtered through Celite, and washed with EtOAc. The filtrate was washed with water and the aqueous phase was extracted three times with EtOAc. The combined organic phases were washed with brine and dried over Na_2SO_4. The mixture was concentrated on a rotary evaporator and the residue was used directly in the next step.

A two-neck flask was charged with K_2CO_3 (1.84 g, 13.3 mmol, 2 equiv) and $Pd(PPh_3)_2Cl_2$ (0.187 g, 0.27 mmol, 4 mol%), and the flask was evacuated and backfilled with argon (three cycles). The residue from the first step was dissolved in dioxane (30 mL) and added to the flask, followed by water (3 mL) and 2-bromo-4-(trifluoromethyl)benzaldehyde **1** (1.0 mL, 6.64 mmol, 1.0 equiv). The mixture was bubbled with argon for 30 min and stirred at 80 °C in an oil-bath for 1 h until the coupling was complete according to ^1H NMR. The reaction mixture was cooled down, filtered through Celite, and washed with EtOAc. The filtrate was washed with water and the aqueous phase was extracted three times with EtOAc. The combined organic phases were washed with brine and dried over Na_2SO_4. The mixture was concentrated on a rotary evaporator and the crude product was purified with flash chromatography (n-hexane/EtOAc 10:1→5:1) affording a yellow oil, which solidified upon standing. The yield of the pale-yellow solid over two steps was 92% (2.11 g, 6.09 mmol). The characterization data was in agreement with the previous literature.[52] ^1H NMR (400 MHz, $CDCl_3$): δ = 9.88 (s, 2H), 8.18 (d, *J* = 8.1 Hz, 2H), 7.93 (dd, *J* = 8.1, 1.8 Hz, 2H), 7.62 (s, 2H); ^{13}C NMR (101 MHz, $CDCl_3$): δ = 189.6, 140.2, 136.8, 135.3 (q, *J* = 33.2 Hz), 130.7, 128.3 (q, *J* = 3.7 Hz), 126.4 (q, *J* = 3.6 Hz), 123.2 (q, *J* = 273.3 Hz).

*Synthesis of **3,6-Bis(trifluoromethyl)-9,10-phenanthrene-quinone (PQ-CF_3)**.* The two-step synthesis was performed using modified literature procedures.[37,42] An oven-dried two-neck flask was

charged with dicarbaldehyde **3** (346 mg, 1.00 mmol, 1.0 equiv) and IMesHCl (34.1 mg, 0.10 mmol, 10 mol%) and the flask was evacuated and backfilled with argon three times. Anhydrous THF (10 mL) was added. The pale-yellow suspension was bubbled with argon for 30 min and stirred at r.t. while DBU (0.16 mL, 1.10 mmol, 1.1 equiv) was added dropwise. Immediate color change from pale-yellow to deep orange was observed (SI, Figure S3). The stirring was continued for 30 min after which the conversion was complete according to ^{1}H NMR. The reaction was quenched with 2 M HCl, and the mixture was extracted three times with EtOAc. The combined organic phases were washed twice with water and brine, and solvents were evaporated. Note! Unnecessary contact of the hydroquinone solution with oxygen should be avoided. A long drying period over a drying agent may increase the risk of oxidative degradation. 3,6-Bis(trifluoromethyl)-9,10-phenanthrenediol (PQH_2-CF_3) was fully characterized from the crude product. ^{1}H NMR (500 MHz, [D6]acetone): $\delta = 9.24$ (s, 2H), 8.92 (s, 2H), 8.48 (d, $J =$ 8.6 Hz, 2H), 7.94 (dd, $J = 8.7$, 1.7 Hz, 2H); ^{13}C NMR (126 MHz, [D6]acetone): $\delta = 137.4$ (*C*OH), 131.0 (*C*CH), 127.0 (q, $J = 31.9$ Hz, *C*CF_3), 126.7 (*C*CH), 125.9 (q, $J = 271.2$ Hz, CF_3), 123.8 (q, $J = 3.5$ Hz, *C*CH), 123.7 (*C*CH), 121.6 (q, $J = 4.3$ Hz, *C*CH); ^{19}F NMR (377 MHz, [D6]acetone): $\delta = -60.78$. HRMS (EI/QMS) *m/z* calcd for $C_{16}H_8F_6O_2$ 346.0428 $[M]^+$; found 346.0434.

The crude product from the previous step was dissolved in DCM (10 mL) under argon and added with degassed aq. 0.11 M $NaIO_4$ (10 mL, 235 mg, 1.10 mmol, 1.1 equiv). The biphasic mixture was stirred vigorously for 5 min at r.t. until the organic phase had turned intense orange (SI, Figure S4). The organic phase was separated, and the aqueous phase was extracted three times with DCM. The combined organics were washed once with water, and the solvent was evaporated. The residue was absorbed in Celite and filtered through silica with 5:1 n-hexane/EtOAc. After evaporation of the solvents, the orange-yellow crystalline solid was obtained in 88% yield (303 mg; 0.88 mmol). $R_f = 0.48$ (5:1 n-hexane/EtOAc); m.p. 174 °C; ^{1}H NMR (400 MHz, $CDCl_3$): $\delta = 8.37$ (d, $J = 8.1$ Hz, 2H), 8.30 (s, 2H), 7.82 (d, $J = 8.1$ Hz, 2H); ^{13}C NMR (101 MHz, $CDCl_3$): $\delta = 178.7$ (C=O), 137.6 (q, $J = 33.2$ Hz, *C*CF_3), 135.3 (*C*CH), 133.2 (*C*CH), 131.6 (*C*CH), 127.1 (q, $J = 3.5$ Hz, *C*CH), 123.2 (q, $J = 273.4$ Hz, CF_3), 121.5 (q, $J = 3.6$ Hz, *C*CH); ^{19}F NMR (377 MHz, $CDCl_3$): $\delta = -64.15$; UV/Vis (MeCN): λ_{max} (ε) = 395 (2200), 314 nm (3000 $mol^{-1}dm^3cm^{-1}$); phosphorescence (1:1 MeCN/CCl_4): $\lambda_{ex} =$ 314 nm; $\lambda_{em} = 582$, 640 nm; HRMS (EI/QMS) *m/z* calcd for $C_{16}H_6F_6O_2$ 344.0272 $[M]^+$; found 344.0259.

General Procedure for the Alcohol Oxidation. Alcohol **4a**–**4ad** (1 equiv), PQ-CF_3 (10 mol%), and 5:1 MeCN/H_2O mixture (5 mL, so that the concentration of the starting material was 0.04 M) were added to a 20 mL vial, which was sealed with a septum. With substrates **4a** and **4b**, PQ (10 mol%) in 7:1 MeCN/H_2O was used. A stock solution of PQ-CF_3 or PQ was freshly prepared and sonicated for 30 min prior to the addition. The reaction mixture was bubbled with O_2 (balloon) for 15 min. The balloon was left attached, and the reaction mixture was stirred and irradiated with blue LEDs (455 nm) at r.t. for the time needed. The reaction mixtures were analyzed with ^{1}H NMR against 1,3,5-trimethoxybenzene as an internal standard to measure the yields shown in Table 2 and Scheme 3. To obtain the isolated yield, aq. $Na_2S_2O_3$ (1 M, 5 mL) was added to the reaction mixture which was then extracted with Et_2O (3×5 mL). The combined organic phases were washed with sat. aq. $NaHCO_3$ (5 mL) and brine (5 mL) and dried over Na_2SO_4. The mixture was concentrated on rotary evaporator and the crude product was purified with flash chromatography (silica gel, 10:1 *n*-pentane/Et_2O).

*4'-Methoxyacetophenone (**5a**).* The product was prepared from **4a** in 0.21 mmol scale using PQ (10 mol%) as the photocatalyst in 7:1 MeCN/H_2O. The reaction time was 15 min. The product was obtained as a pale-yellow oil in 92% (29.1 mg, 0.19 mmol) yield. The characterization data was in agreement with the previous literature.[53] ^{1}H NMR (400 MHz, $CDCl_3$): $\delta = 7.94$ (d, $J = 8.9$ Hz, 1H), 6.93 (d, $J = 8.9$ Hz, 1H), 3.87 (s, 3H), 2.55 (s, 3H); ^{13}C NMR (101 MHz, $CDCl_3$): $\delta = 196.9$, 163.6, 130.7, 130.4, 113.8, 55.6, 26.4.

*Large Scale Synthesis of **5a**.* The product **5a** was prepared from **4a** in 1.00 mmol scale using PQ (10 mol%) as the photocatalyst in 7:1 MeCN/H_2O (10 mL). The conversion was complete after 2 h. The yield of **5a** was 88% (133 mg, 0.89 mmol).

*4'-Bromoacetophenone (**5e**).* The product was prepared from **4e** in 0.20 mmol scale with the reaction time of 1 h. The product was obtained as a white solid in 94% (37.7 mg, 0.19 mmol) yield. The characterization data was in agreement with the previous literature.[53] ^{1}H NMR (400 MHz, $CDCl_3$): $\delta = 7.82$ (d, $J = 8.7$ Hz, 2H), 7.60 (d, $J = 8.6$ Hz, 2H), 2.58 (s, 3H); ^{13}C NMR (101 MHz, $CDCl_3$): $\delta =$ 197.2, 136.0, 132.0, 130.0, 128.4, 26.7.

*Large Scale Synthesis of **5e**.* The product **5e** was prepared from **4e** in 1.01 mmol scale in 5:1 MeCN/H_2O (10 mL). The conversion was complete after 3 h. The yield of **5e** was 95% (192 mg, 0.96 mmol).

Supporting Information

Further experimental and computational details, NMR, UV-Vis, and phosphorescence spectra as well as CV and XRD data can be found in the Supporting Information.

Deposition Number CCDC 2195837 (PQ-CF_3) contains the supplementary crystallographic data for this paper. These data are provided free of charge by the joint Cambridge Crystallographic Data Centre and Fachinformationszentrum Karlsruhe Access Structures service.

The authors have cited additional references within the Supporting Information.[54–68]

Acknowledgements

The Finnish National Centre for Scientific Computing (CSC) is recognized for computational resources. Gudrun Silvennoinen (Department of Chemistry, University of Helsinki) is acknowledged for performing high-resolution mass spectrometry. This work was supported by ERC Consolidator Grant Project PADRE, decision number 101001016.

Conflict of Interests

The authors declare no conflict of interest.

Data Availability Statement

The data that support the findings of this study are available in the supplementary material of this article.

Keywords: alcohol oxidation · hydrogen transfer · phenanthrenequinone · photocatalysis · photooxidation

[1] N. L. Reed, T. P. Yoon, *Chem. Soc. Rev.* **2021**, *50*, 2954–2967.
[2] J. S. Winterle, D. S. Kliger, G. S. Hammond, *J. Am. Chem. Soc.* **1976**, *98*, 3719–3721.
[3] N. A. Romero, D. A. Nicewicz, *Chem. Rev.* **2016**, *116*, 10075–10166.
[4] M. V. Bobo, J. J. I. Kuchta, A. K. Vannucci, *Org. Biomol. Chem.* **2021**, *19*, 4816–4834.
[5] T. Bortolato, S. Cuadros, G. Simionato, L. Dell'Amico, *Chem. Commun.* **2022**, *58*, 1263–1283.
[6] A. Joshi-Pangu, F. Lévesque, H. G. Roth, S. F. Oliver, L.-C. Campeau, D. Nicewicz, D. A. DiRocco, *J. Org. Chem.* **2016**, *81*, 7244–7249.
[7] A. R. White, L. Wang, D. A. Nicewicz, *Synlett* **2019**, *30*, 827–832.
[8] B. Zilate, C. Fischer, C. Sparr, *Chem. Commun.* **2020**, *56*, 1767–1775.
[9] J. Mateos, F. Rigodanza, A. Vega-Peñaloza, A. Sartorel, M. Natali, T. Bortolato, G. Pelosi, X. Companyó, M. Bonchio, L. Dell'Amico, *Angew. Chem. Int. Ed.* **2020**, *59*, 1302–1312.
[10] E. Speckmeier, T. G. Fischer, K. Zeitler, *J. Am. Chem. Soc.* **2018**, *140*, 15353–15365.
[11] A. Vega-Peñaloza, J. Mateos, X. Companyó, M. Escudero-Casao, L. Dell'Amico, *Angew. Chem. Int. Ed.* **2021**, *60*, 1082–1097.
[12] J. A. Dantas, J. T. M. Correia, M. W. Paixão, A. G. Corrêa, *ChemPhotoChem* **2019**, *3*, 506–520.
[13] A. Itoh, in *Photoorganocatalysis Org. Synth.* (Eds.: M. Fagnoni, S. Protti, D. Ravelli), World Scientific (Europe), **2019**, pp. 39–70.
[14] J. Cervantes-González, D. A. Vosburg, S. E. Mora-Rodriguez, M. A. Vázquez, L. G. Zepeda, C. Villegas Gómez, S. Lagunas-Rivera, *ChemCatChem* **2020**, *12*, 3811–3827.
[15] S. Jana, A. Verma, R. Kadu, S. Kumar, *Chem. Sci.* **2017**, *8*, 6633–6644.
[16] J. Rostoll-Berenguer, G. Blay, J. R. Pedro, C. Vila, *Catalysts* **2018**, *8*, 653.
[17] P. Natarajan, D. Chuskit, Priya, Manjeet, *ChemistrySelect* **2021**, *6*, 11838–11844.
[18] P. Natarajan, D. Chuskit, Priya, Manjeet, *New J. Chem.* **2022**, *46*, 322–327.
[19] J. Talvitie, I. Alanko, E. Bulatov, J. Koivula, T. Pöllänen, J. Helaja, *Org. Lett.* **2022**, *24*, 274–278.
[20] J. Rostoll-Berenguer, F. J. Sierra-Molero, G. Blay, J. R. Pedro, C. Vila, *Adv. Synth. Catal.* **2022**, *364*, 4054–4060.
[21] Y. Zhang, P. Ji, W. Hu, Y. Wei, H. Huang, W. Wang, *Chem. A Eur. J.* **2019**, *25*, 8225–8228.
[22] H. Wang, T. Li, D. Hu, X. Tong, L. Zheng, C. Xia, *Org. Lett.* **2021**, *23*, 3772–3776.
[23] M. Wang, J. Liu, Y. Zhang, P. Sun, *Adv. Synth. Catal.* **2022**, *364*, 2660–2665.
[24] M. Wang, Y. Zhang, X. Yang, P. Sun, *Org. Biomol. Chem.* **2022**, *20*, 2467–2472.
[25] M. E. Peover, *J. Chem. Soc.* **1962**, 4540–4549.
[26] S. Samanta, P. Biswas, *RSC Adv.* **2015**, *5*, 84328–84333.
[27] W. Schilling, D. Riemer, Y. Zhang, N. Hatami, S. Das, *ACS Catal.* **2018**, *8*, 5425–5430.
[28] N. F. Nikitas, D. I. Tzaras, I. Triandafillidi, C. G. Kokotos, *Green Chem.* **2020**, *22*, 471–477.
[29] A. K. Bains, Y. Ankit, D. Adhikari, *ChemSusChem* **2021**, *14*, 324–329.
[30] S. Ma, J.-W. Cui, C.-H. Rao, M.-Z. Jia, Y.-R. Chen, J. Zhang, *Green Chem.* **2021**, *23*, 1337–1343.
[31] M. Shee, N. D. P. Singh, *Adv. Synth. Catal.* **2022**, *364*, 2032–2039.
[32] J. Zhao, Z. Luo, Y. Liu, J. Xu, Z. Huang, W. Xiong, *Tetrahedron* **2023**, *131*, 133208.
[33] S. Trosien, S. R. Waldvogel, *Org. Lett.* **2012**, *14*, 2976–2979.
[34] S. Halbedl, M.-C. Kratzer, K. Rahm, N. Crosta, K.-S. Masters, J. Zippert, S. Bräse, D. Gradl, *FEBS Lett.* **2013**, *587*, 522–527.
[35] K. Urakawa, M. Sumimoto, M. Arisawa, M. Matsuda, H. Ishikawa, *Angew. Chem. Int. Ed.* **2016**, *55*, 7432–7436.
[36] Y.-K. Zhang, C. Liu, C. M. Hahne, G. L. Steere, C. Y. Liu, *Boron Containing Compounds and Their Uses*, **2022**, WO2022040157 A1.
[37] K. Satyam, J. Ramarao, S. Suresh, *Org. Biomol. Chem.* **2021**, *19*, 1488–1492.
[38] D. Enders, O. Niemeier, *Synlett* **2004**, *2004*, 2111–2114.
[39] K. Urakawa, M. Sumimoto, M. Arisawa, M. Matsuda, H. Ishikawa, *Angew. Chem. Int. Ed.* **2016**, *55*, 7432–7436.
[40] X. Wang, R.-X. Chen, Z.-F. Wei, C.-Y. Zhang, H.-Y. Tu, A.-D. Zhang, *J. Org. Chem.* **2016**, *81*, 238–249.
[41] Y. Sawaki, C. S. Foote, *J. Am. Chem. Soc.* **1983**, *105*, 5035–5040.
[42] M. Y. Zhang, R. A. Barrow, *Org. Lett.* **2017**, *19*, 2302–2305.
[43] D. M. Togashi, D. E. Nicodem, *Spectrochim. Acta Part A* **2004**, *60*, 3205–3212.
[44] V. V. Pavlishchuk, A. W. Addison, *Inorg. Chim. Acta* **2000**, *298*, 97–102.
[45] S. Fukuzumi, S. Itoh, T. Komori, T. Suenobu, A. Ishida, M. Fujitsuka, O. Ito, *J. Am. Chem. Soc.* **2000**, *122*, 8435–8443.
[46] S. Wu, Q. Zhao, C. Wu, C. Wang, H. Lei, *Org. Chem. Front.* **2022**, *9*, 2593–2599.
[47] H. Wang, J. Ni, Y. Zhang, *Tetrahedron Lett.* **2022**, *104*, 154021.
[48] M. B. Smith, J. March, in *March's Adv. Org. Chem.*, John Wiley & Sons, Ltd, **2007**, pp. 395–416.
[49] E. M. Simmons, J. F. Hartwig, *Angew. Chem. Int. Ed.* **2012**, *51*, 3066–3072.
[50] D. R. Weinberg, C. J. Gagliardi, J. F. Hull, C. F. Murphy, C. A. Kent, B. C. Westlake, A. Paul, D. H. Ess, D. G. McCafferty, T. J. Meyer, *Chem. Rev.* **2012**, *112*, 4016–4093.
[51] E. A. Ison, A. Ison, *J. Chem. Educ.* **2012**, *89*, 1575–1577.
[52] Q. Xia, X. Zhao, J. Zhang, J. Wang, G. Song, *Tetrahedron Lett.* **2020**, *61*, 151500.
[53] F. Li, N. Wang, L. Lu, G. Zhu, *J. Org. Chem.* **2015**, *80*, 3538–3546.
[54] J. Mangas-Sánchez, M. Rodríguez-Mata, E. Busto, V. Gotor-Fernández, V. Gotor, *J. Org. Chem.* **2009**, *74*, 5304–5310.
[55] J. Liu, S. Yang, W. Tang, Z. Yang, J. Xu, *Green Chem.* **2018**, *20*, 2118–2124.
[56] S. R. Roy, S. C. Sau, S. K. Mandal, *J. Org. Chem.* **2014**, *79*, 9150–9160.
[57] F. Puls, P. Linke, O. Kataeva, H.-J. Knölker, *Angew. Chem. Int. Ed.* **2021**, *60*, 14083–14090.
[58] S. S. Ribeiro, C. Raminelli, A. L. M. Porto, *J. Fluorine Chem.* **2013**, *154*, 53–59.
[59] R. Zhong, Z. Wei, W. Zhang, S. Liu, Q. Liu, *Chem* **2019**, *5*, 1552–1566.
[60] J.-L. Yu, H. Wang, K.-F. Zou, J.-R. Zhang, X. Gao, D.-W. Zhang, Z.-T. Li, *Tetrahedron* **2013**, *69*, 310–315.
[61] J. Zhang, G. Lu, C. Cai, *Green Chem.* **2017**, *19*, 4538–4543.
[62] Á. García-Muñoz, A. I. Ortega-Arizmendi, M. A. García-Carrillo, E. Díaz, N. Gonzalez-Rivas, E. Cuevas-Yañez, *Synlett* **2012**, *44*, 2237–2242.
[63] C. W. Anson, S. S. Stahl, *J. Am. Chem. Soc.* **2017**, *139*, 18472–18475.
[64] G. M. Sheldrick, *Acta Crystallogr. Sect. A* **2015**, *71*, 3–8.
[65] G. M. Sheldrick, *Acta Crystallogr. Sect. C* **2015**, *71*, 3–8.
[66] M. J. Frisch, G. W. Trucks, H. B. Schlegel, G. E. Scuseria, M. A. Robb, J. R. Cheeseman, G. Scalmani, V. Barone, G. A. Petersson, H. Nakatsuji, X. Li, M. Caricato, A. V. Marenich, J. Bloino, B. G. Janesko, R. Gomperts, B. Mennucci, D. J. Hratch, Gaussian 16. Gaussian, Inc., Wallingford CT 2016.
[67] H. G. Roth, N. A. Romero, D. A. Nicewicz, *Synlett* **2016**, *27*, 714–723.
[68] P. C. St. John, Y. Guan, Y. Kim, S. Kim, R. S. Paton, *Nat. Commun.* **2020**, *11*, 1–12.

Manuscript received: May 25, 2023
Revised manuscript received: June 21, 2023
Accepted manuscript online: June 22, 2023
Version of record online: June 22, 2023

RESEARCH ARTICLE

We designed a synthetic route for previously unpublished photocatalyst, 3,6-bis(trifluoromethyl)-9,10-phenanthrenequinone (PQ-CF_3), and studied its photophysical properties in comparison with other known phenanthrenequinones. The photocatalytic efficacy was demonstrated in the oxidation of 29 secondary alcohols. Mechanistic studies revealed that regardless of the electronic properties of the substrate, PQ-CF_3 operates rather via highly efficient hydrogen atom transfer (HAT) than single-electron transfer (SET).

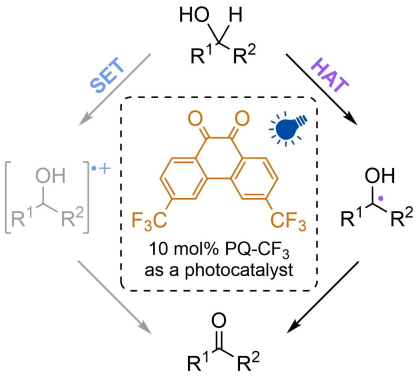

*J. Talvitie, I. Alanko, Dr. A. Lenarda, Dr. N. Durandin, Prof. Dr. N. Tkachenko, Dr. M. Nieger, Dr. J. Helaja**

1 – 10

Electron-Deficient Phenanthrenequinone Derivative for Photoactivated Hydrogen Atom Transfer Mediated Oxidation of Secondary Alcohols